

SNAIL Regulates Interleukin-8 Expression, Stem Cell–Like Activity, and Tumorigenicity of Human Colorectal Carcinoma Cells

WEI-LUN HWANG,^{*,‡,§} MUH-HWA YANG,^{||,¶} MING-LONG TSAI,^{||,¶} HSIN-YI LAN,^{||} SHU-HAN SU,^{*} SHIH-CHING CHANG,^{**} HAO-WEI TENG,^{||,¶} SHUNG-HAUR YANG,^{**} YUAN-TZU LAN,^{||,**} SHIH-HWA CHIOU,^{||,¶} and HSEI-WEI WANG^{*,§,||,‡,§§}

^{*}Institution of Microbiology and Immunology, [‡]Institution of Biochemistry and Molecular Biology, ^{||}Institute of Clinical Medicine, and ^{‡‡}VGH-YM Genome Research Center, National Yang-Ming University, Taipei; [§]Molecular Medicine Program, Taiwan International Graduate Program, Institute of Biomedical Sciences, Academia Sinica, Taipei; [¶]Division of Hemato-Oncology, Department of Internal Medicine, ^{¶¶}Department of Medical Research and Education, and ^{**}Division of Colon & Rectal Surgery, Department of Surgery, Taipei Veterans General Hospital, Taipei, Taiwan; and ^{§§}Department of Education and Research, Taipei City Hospital, Taipei, Taiwan

BACKGROUND & AIMS: Some cancer cells have activities that are similar to those of stem cells from normal tissues, and cell dedifferentiation correlates with poor prognosis. Little is known about the mechanisms that regulate the stem cell–like features of cancer cells; we investigated genes associated with stem cell–like features of colorectal cancer (CRC) cells. **METHODS:** We isolated colonospheres from primary CRC tissues and cell lines and characterized their gene expression patterns by microarray analysis. We also investigated the biological features of the colonosphere cells. **RESULTS:** Expanded CRC colonospheres contained cells that expressed high levels of CD44 and CD166, which are markers of colon cancer stem cells, and had many features of cancer stem cells, including chemoresistance and radioresistance, the ability to initiate tumor formation, and activation of epithelial-mesenchymal transition (EMT). SNAIL, an activator of EMT, was expressed at high levels by CRC colonospheres. Overexpression of Snail in CRC cells induced most properties of colonospheres, including cell dedifferentiation. Two hundred twenty-seven SNAIL-activated genes were up-regulated in colonospheres; gene regulatory networks centered around interleukin (IL)-8 and JUN. Blocking IL-8 expression or activity disrupted SNAIL-induced stem cell–like features of colonospheres. We observed that SNAIL activated the expression of *IL8* by direct binding to its E3/E4 E-boxes. In CRC tissues, SNAIL and IL-8 were coexpressed with the stem cell marker CD44 but not with CD133 or CD24. **CONCLUSIONS:** In human CRC tissues, SNAIL regulates expression of IL-8 and other genes to induce cancer stem cell activities. Strategies that disrupt this pathway might be developed to block tumor formation by cancer stem cells.

Keywords: Colon Cancer; Tumor Development; Systems Biology; Gene Regulation.

Colorectal cancer (CRC) is one of the most common cancers worldwide. Reevaluating our current knowledge of CRC and developing novel therapeutic strategies is still crucial. Evidence suggests that cancer cells possess characteristics reminiscent of those of normal stem cells.¹ Unveiling the genes responsible for CRC cell stemness and

chemoradioresistance should lead to novel therapeutic approaches.

The epithelial-mesenchymal transition (EMT) is a critical process involved in the transdifferentiation of polarized epithelial cells into an invasive mesenchymal phenotype.² The EMT also contributes to the acquisition of stem cell traits in breast cancer cells and the generation of cells with features similar to breast cancer stem cells.^{3,4} These results have provided a crucial link between metastasis and stem cell properties. One of the major EMT regulators is the zinc-finger transcription factor family protein Snail.^{5,6} The critical roles of Snail in CRC have been previously identified; this involves Snail enhancing the degradation of prostaglandin E₂, which promotes cancer progression.⁷ Snail also contributes to the down-regulation of E-cadherin and the vitamin D receptor in colon cancer, which results in the failure of vitamin D analogue treatment.^{8,9} Expression of Snail correlates with poor patient prognosis in CRC.¹⁰ In breast cancer, Snail promotes stemness and generates mammosphere cells.³ How Snail induces dedifferentiation is unclear, and whether Snail can introduce similar stemness traits in CRC is also undecided. Because Snail or other EMT transcription factors are nontargetable by current therapeutic approaches, the identification of Snail-regulated genes that can be targeted by drugs may lead to the development of novel therapeutic strategies against EMT-related malignancy.

Materials and Methods

Tissue Collection and Colonosphere Expansion

This study was approved by the Institutional Ethics Committee/Institutional Review Board of the Taipei Veterans General Hospital. A total of 22 primary colorectal specimens from individuals aged 42 to 90 years with disease grade 2 to 3 and American Joint Committee on Cancer stage IIA to IVB were collected during surgery

Abbreviations used in this paper: bFGF, basic fibroblast growth factor; CRC, colorectal cancer; EGF, epidermal growth factor; EMT, epithelial-mesenchymal transition; IL, interleukin; nAb, neutralizing antibody; qPCR, quantitative polymerase chain reaction.

© 2011 by the AGA Institute

0016-5085/\$36.00

doi:10.1053/j.gastro.2011.04.008

(Supplementary Table 1). These samples were immersed in normal saline, brought to the laboratory within 1 hour, and washed 5 times with phosphate-buffered saline containing 500 U/mL penicillin and 500 μ g/mL streptomycin (Gibco, Carlsbad, CA). Samples of each solid tissue were then immersed in TRIzol reagent (Invitrogen, Carlsbad, CA) for RNA isolation. Other samples from each tissue were immersed in 4% paraformaldehyde (Sigma, St Louis, MO) to allow the preparation of paraffin-embedded blocks. Finally, the remaining samples were minced into small fragments (2 mm³) for primary culture. These tissue fragments were washed in 100 mmol/L phosphate buffer (pH 7.0) with 6.5 mmol/L dithiothreitol (Sigma) for 15 minutes at room temperature to avoid mucus contamination.¹¹ After removal of dithiothreitol solution and additional washing with phosphate-buffered saline, the tissue fragments were resuspended in serum-free Dulbecco's modified Eagle medium/F12 (Gibco) supplemented with 500 U/mL penicillin-streptomycin and 1.5 mg/mL type IV collagenase (Sigma) for enzymatic dissociation at 37°C for 1 hour. The cells were mechanically broken apart by pipetting every 15 minutes during digestion. Released cell samples were subjected to fluorescence-activated cell sorter analysis, while the remaining cells were cultured using type I collagen-coated (Sigma) plates in RPMI 1640 or Dulbecco's modified Eagle medium (Gibco) supplemented with 10% fetal bovine serum (Gibco) and 1% penicillin-streptomycin to obtain primary cells. Some released cell samples were cultured in stem cell medium (Dulbecco's modified Eagle medium/F12 supplemented with N₂ Plus Supplement [R&D Systems, Minneapolis, MN], 10 ng/mL recombinant basic fibroblast growth factor [bFGF; PeproTech Asia; Rehovot, Israel], 10 ng/mL epidermal growth factor [EGF; PeproTech Asia], and 1% penicillin-streptomycin) to obtain colonospheres.¹²

To obtain colonospheres from the cancer cell lines, dissociated cells were cultured in stem cell medium for at least 2 weeks.¹² To enhance *in vitro* epithelial differentiation, suspended colonospheres were collected by centrifugation and cultured in Dulbecco's modified Eagle medium supplemented with 1% fetal bovine serum¹³ and the resultant epithelial-like cells were named sphere-derived adherent cells. TrypLE Express (Invitrogen) was used to separate cells from the centrifuge-collected colonospheres and adherent cells to allow cell counting and other experiments.

Miscellaneous Methods

For other methods, please refer to the Supplementary Materials and Methods.

Results

Enhanced Malignancy in CD44⁺ CRC Colonospheres Expanded by Culture Under Serum-Free Conditions

Self-renewal capability is a major property of stem cells, and spheroid formation is a self-renewal index.³ Culture under bFGF(+)/EGF(+) serum-free conditions has been

used to expand stem-like spheroid cells from primary CRC tissue.¹⁴⁻¹⁶ Primary cells derived from the bFGF(+)/EGF(+) serum-free culture more faithfully mirror the original gene expression profiles and tumor morphology of the cells.¹⁷ We expanded the cancer stem cells as colonospheres from primary CRC specimens and also assessed the sphere formation ability of 5 CRC cell lines. CRC colonospheres were obtained by expansion from a large subset of specimens (16/22; Supplementary Figure 1A and Supplementary Table 1). However, only the HT29 and HCT15 cell lines formed significant spheroid bodies reminiscent of primary colonospheres after 3 weeks of culture (first colonospheres) (Supplementary Figure 1B). The expanded primary colonospheres were positive for A33, which is expressed in almost all colonic epithelium irrespective of differentiation status^{18,19} (Supplementary Figure 2). These CRC colonospheres originated from a single cell rather than having developed by mere cell aggregation (Supplementary Figure 1C).

CD44, CD24, CD166, CD133 and aldehyde dehydrogenase 1 (ALDH1) have all been proposed as markers of CRC cancer stem cells.²⁰ In this context, the existence of various cancer stem cell populations in isolated colonospheres was evaluated. CD44⁺, CD24⁺, CD133⁺, or CD166⁺ population was enriched in primary colonospheres (Figure 1A and Supplementary Figure 3B and C, patients 7 and 8). CD44⁺, CD24⁺, or CD166⁺ population was also enriched in HT29-derived or HCT15-derived colonospheres (Figure 1A and Supplementary Figure 3A). After spheroid cultivation, the CD44⁺ and CD166⁺ populations were most consistently enriched among the expanded colonospheres (Figure 1A).

To compare relative malignancy between the expanded colonospheres and the putative cancer stem cell populations of sorted and unsorted parental cells (Supplementary Figure 3E and F), as well as colonospheres derived from various sorted populations, these were subjected into soft agar assay and a spheroid-forming assay. CD44⁺ cells formed more colonies and spheroids than CD44⁻ cells. However, double sorting with either for CD24 or CD133 did not further increase the number of malignant cells (Figure 1B and C). Colonosphere cells formed more colonies and spheroids than CD44⁺ cells (Figure 1B and C). Colonospheres from presorted CD44⁺ or CD133⁺ parental cells were not more malignant than spheres from nonsorted cells (Figure 1B and C). Colonospheres also harbored enhanced tumorigenicity *in vivo* (Supplementary Figure 4A). Serum-free culture is therefore one useful approach to expanding malignant CRC stem-like cells.

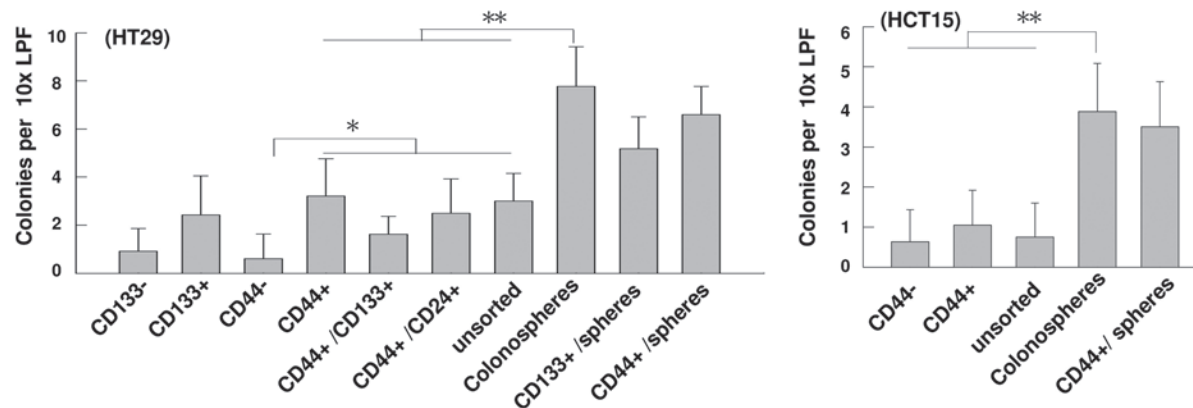
CRC Spheres Inherit Stem Cell Properties

Because malignant cells harbor more stemness traits,¹ we examined stem cell and differentiation markers in the colonospheres. Sphere-derived adherent cells exhibited epithelial-like morphology on serum exposure (Supplementary Figure 1D). Compared with parental cells or sphere-derived adherent cells, the expression levels of various stemness genes in colonospheres were significantly higher, whereas those of the differentiation markers CDX2 and BMP4 were lower (Figure 2A and Supplementary Figure 4B).

A

CSCs markers	HT29		HCT15		CRC pt #8		CRC pt #7	
	monolayer (%)	colonosphere (%)	monolayer (%)	colonosphere (%)	monolayer (%)	colonosphere (%)	monolayer (%)	colonosphere (%)
CD44	64.20 ± 5.23	88.95 ± 4.15	49.17 ± 6.24	81.13 ± 1.18	39.12 ± 3.11	71.58 ± 6.87	25.62 ± 4.51	47.12 ± 4.15
CD24	25.12 ± 4.23	41.65 ± 5.73	0.34 ± 3.29	0.17 ± 2.88	1.03 ± 2.97	87.94 ± 4.61	4.44 ± 4.23	7.57 ± 5.73
CD166	10.96 ± 2.48	19.53 ± 4.78	18.41 ± 5.39	67.20 ± 4.21	45.67 ± 5.16	84.72 ± 3.63	6.54 ± 3.09	34.87 ± 7.41
CD133	11.08 ± 5.32	16.86 ± 3.28	0.11 ± 1.24	0.09 ± 1.37	2.18 ± 3.35	69.71 ± 5.59	8.93 ± 4.22	3.54 ± 3.14
CD44+/CD24+	17.34 ± 2.74	33.14 ± 4.11	0.39 ± 3.14	0.30 ± 2.37	4.15 ± 3.67	79.55 ± 6.13	NA	NA
CD44+/CD133+	4.87 ± 5.29	16.53 ± 2.47	0.53 ± 2.18	1.21 ± 2.45	5.24 ± 4.28	63.84 ± 5.68	2.11 ± 2.45	2.15 ± 2.47
CD133+/CD24+	11.47 ± 2.46	16.09 ± 1.53	0.38 ± 1.17	0.19 ± 2.62	1.23 ± 3.28	85.77 ± 6.45	0.19 ± 2.62	2.09 ± 1.53
ALDH activity	33.97 ± 5.11	54.57 ± 7.49	43.04 ± 6.71	23.73 ± 4.56	NA	NA	NA	NA

B



C

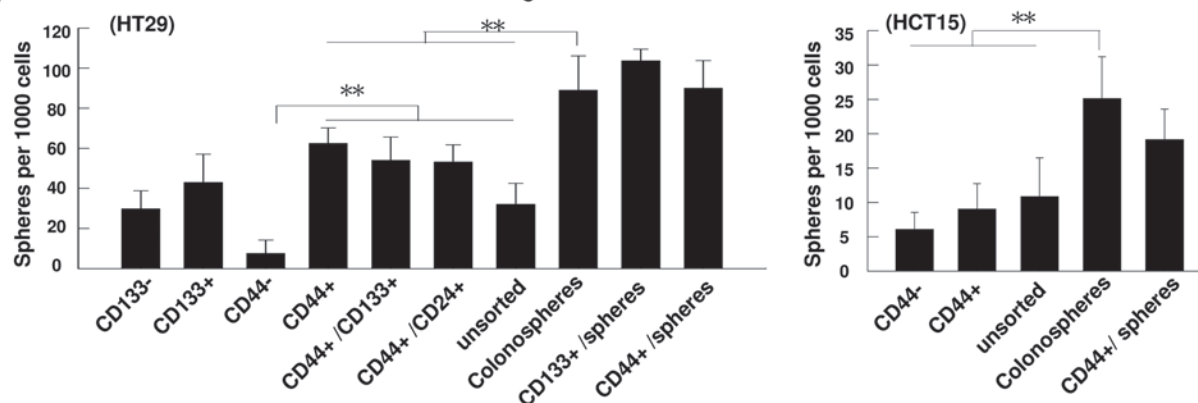


Figure 1. Characterization of the CRC colonospheres expanded by defined medium cultivation. (A) Flow cytometry analysis of putative cancer stem cell markers on parental cells and colonospheres from CRC cell lines (HT29, HCT15) and primary cells (patients 7–8). NA, not assessed. (B and C) The relative anchorage-independent (B) colony-forming and (C) spheroid-forming abilities of sorted parental cells, unsorted parental cells, and colonospheres expanded using defined medium culture. * $P < .05$; ** $P < .01$.

Stem-like colonospheres had a greater self-renewal ability compared with parental cells and sphere-derived adherent cells, as indexed the formation of second spheres (Figure 2B and Supplementary Figure 4C, left). In addition, sphere cells formed more colonies in soft agar (Figure 2C and Supplementary Figure 4C, right) and more efficiently produced bulky tumors in xenotransplanted mice (Figure 2D and Supplementary Figure 4D). Injected colonospheres differentiated in vivo, showing the appearance of goblet cells with mucous-secreting granules (Alcian blue-positive staining) in xenograft tumors (Supplementary Figure 4E, left) as well as re-expressing CDX2 (Supplementary Figure 4E, right). Colonosphere cells also showed greater resistance to chemotherapy/radiotherapy as assessed by treatment with 5-fluoro-

uracil and Co-60 irradiation, respectively (Figure 2E). Furthermore, colonospheres showed higher motility (Supplementary Figure 4F) and higher in vivo hepatic and pulmonary metastatic ability (Figure 2F).

Snail Is Overexpressed in Colonospheres and Is Sufficient and Essential for the Introduction of Stemness and Malignancy Traits Into CRC Cells

To explore the molecules governing stemness and tumorigenicity in CRC colonospheres, we examined their transcriptome profile. A total of 7134 probe sets were specifically up-regulated or down-regulated in CRC colonospheres (Figure 3A and Supplementary Table 2).

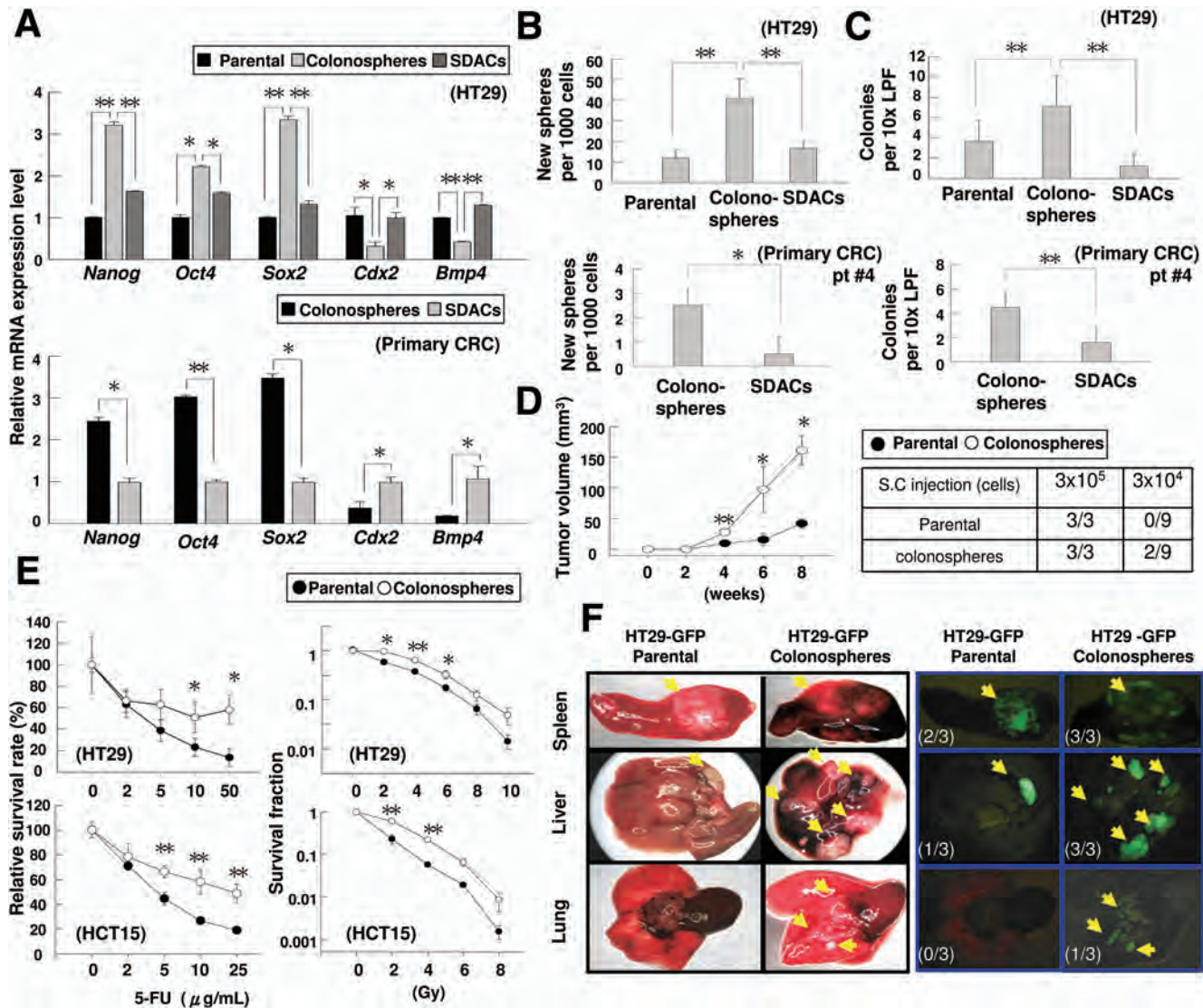


Figure 2. Inherited stem cell properties and tumor malignancy in CRC colonospheres. (A) Reverse-transcription qPCR validation of stemness gene expression in CRC cell lines and primary cells (patients 2, 3, 4, 9). The mean expression levels of the target genes were compared with that of a GAPDH control. Results are expressed as mean \pm SD. * $P < .05$; ** $P < .01$. (B) Spheres formed per 1000 seeded cells as an index of cell renewal ability. (C) Colonies formed per 5000 seeded cells in a soft agar assay as an index of in vitro tumorigenicity. (D) Enhanced in vivo tumorigenicity of colonospheres. (Left) Increased tumor volume in mice at a dose of 3×10^5 cells using HT29-GFP colonospheres. (Right) Enhanced tumor-initiating potential associated with HT29-GFP colonospheres in mice. (E) Increased chemoresistance (left) and radioresistance (right) of the colonospheres. (F) Enhanced in vivo metastatic capability of HT29-GFP colonospheres. Cells were injected into the subcapsular region of nude mouse spleen. Mice were killed 12 weeks after implantation ($n = 3$).

The colonosphere-enriched genes were subjected to a Gene Ontology (GO) database search²¹ to find statistically overrepresented functional groups ($P < .05$; Figure 3A). The predominant processes up-regulated in the colonospheres include those pertaining to cell growth, apoptosis, cell motility and adhesion, as well as those involved in ectoderm or epidermis development (Figure 3A). One of the most abundant factors in colonospheres was SNAIL (Snail), which is a highly important EMT transcription factor^{5,6} ($q = 0.001833$; Figure 3A). The expression levels of interleukin (IL)-8 and vascular endothelial growth factor were also significantly higher (Figure 3A). The abundant expression of these genes in primary and cell line-derived colonospheres was validated by quantitative

polymerase chain reaction (qPCR) (Figure 3A, right panel). The occurrence of EMT is evidenced by down-regulation of E-cadherin together with up-regulation of N-cadherin during colonosphere formation (Supplementary Figure 5A). Furthermore, Snail expression is significantly higher in CD44⁺ HT29 colonospheres than in CD44⁻ colonospheres (not shown). Snail was also found to be up-regulated in spheroids derived from HTB186 medulloblastoma cells and FaDu human head and neck cancer cells (Figure 3B), indicating a universal role for Snail in functioning of tumor cancer stem cells. However, the messenger RNA levels of another 2 critical EMT regulators, Slug (SNAIL2) and Twist1, which were not in our up-regulated/down-regulated gene list, were not increased

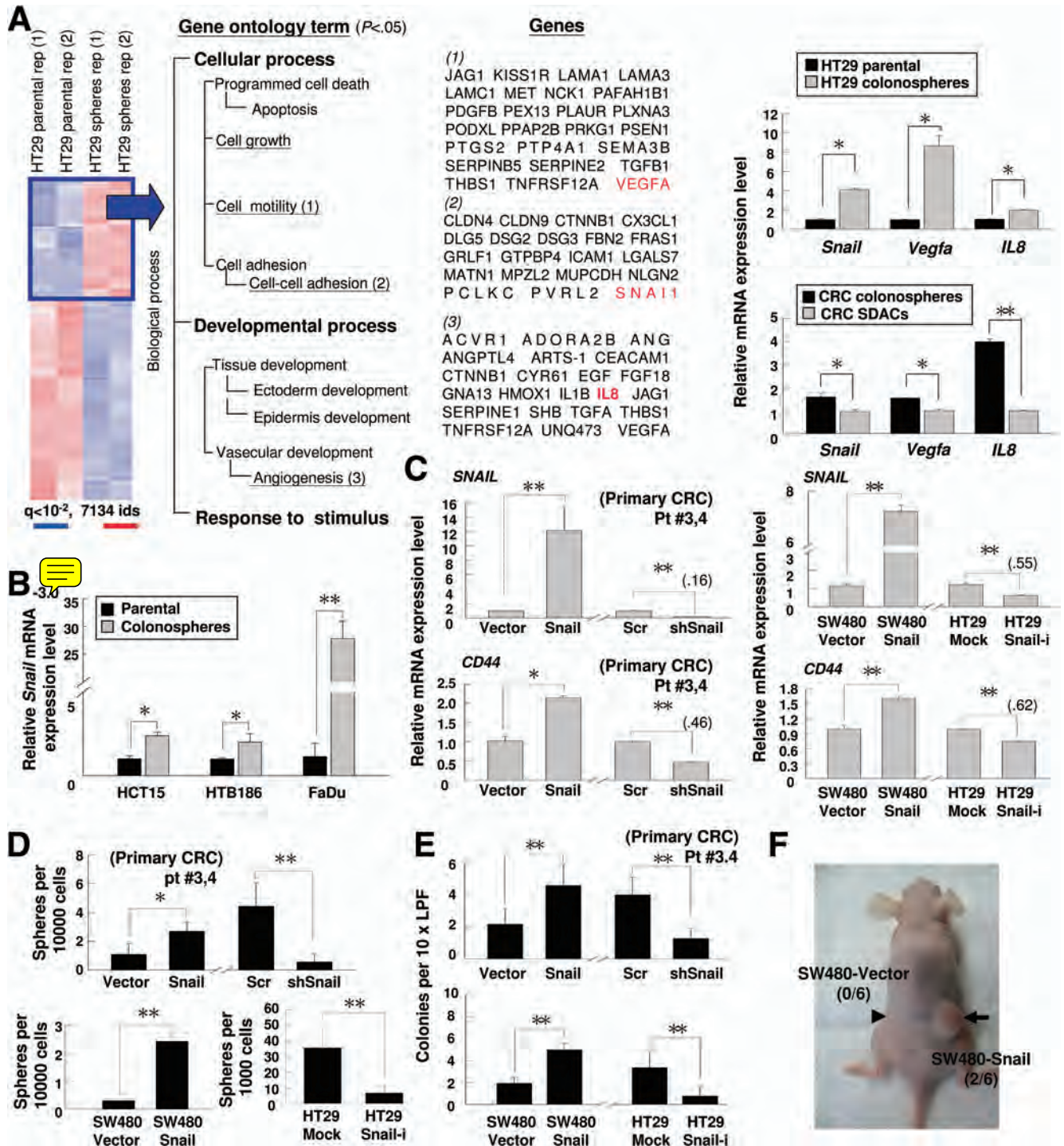


Figure 3. Snail is sufficient and essential for CRC cell self-renewal and malignancy. (A) A heat map shows the differentially expressed genes in colonospheres (positive false discovery rate $q < .01$). (Left) Genes in red, increased expression; in blue, decreased expression. Selected genes inside 3 Gene Ontology categories ($P < .05$) are listed. (Right) Reverse-transcription qPCR validation of genes marked by red (left) in HT29 and primary CRC cells (patients 3, 4, 14). (B) Reverse-transcription qPCR validation of Snail expression in HCT15, HTB186 (medulloblastoma), and FaDu (head and neck cancer) spheroids. * $P < .05$; ** $P < .01$. (C) Relative Snail and CD44 expression levels in primary CRC cells (patients 3-4) (left) and CRC cell lines (right) upon ectopic Snail expression or knocked down. (D) Spheres formed per seeded cell from Snail ectopic-expressing primary cells, Snail-depleted primary colonospheres (patients 3-4) (upper), SW480-Snail cells, and Snail-depleted HT29 cells (lower). (E) Fold changes in colony numbers measured by anchorage-independent soft agar assays in Snail ectopic-expressing primary cells, Snail-depleted primary colonospheres (patients 3-4) (upper), SW480-Snail cells, and Snail-depleting HT29 cells (lower). (F) Ectopic Snail expression enhances tumorigenicity. A total of 1×10^6 cells of SW480-Vector and SW480-Snail cells were implanted subcutaneously into both flanks of a nude mice host.

in colonospheres when examined by qPCR and immunoblotting (not shown).

Snail alone is able to enhance cancer cell self-renewal and has been shown to induce the creation of stem-like mammospheres from transformed mammary epithelial cells.³ A similar scenario would seem to also occur in transformed colorectal cells. The stable overexpression of Snail in SW480 cells resulted in a higher self-renewal ability, as shown by greater colonosphere formation, while knockdown of Snail in HT29 cells resulted in the breakdown of colonospheres (Supplementary Figure 5B). The transient overexpression of Snail in primary colonospheres, or stably in SW480 or HCT15 CRC cells, also induced the expression of the CD44 stem cell marker, while the knockdown of Snail in primary CRC colonospheres or HT29 cells diminished CD44 messenger RNA (Figure 3C and Supplementary Figure 5C). CRC cells that had undergone the EMT due to overexpression of Snail showed higher self-renewal ability because they formed more first sphere cells (Figure 3D and Supplementary Figure 5D). Snail also induced tumorigenicity in vitro and in vivo, forming more colonies in soft agar (Figure 3E and Supplementary Figure 5E) and more tumors in nude mice (Figure 3F). This enhanced self-renewal/malignancy as a result of Snail overexpression would seem also to cause induction of chemoradioresistance. Indeed, cells expressing higher levels of Snail were more resistant to 5-fluorouracil treatment and Cobalt-60 irradiation, while knockdown of Snail expression in HT29 cells reversed such resistance (Supplementary Figure 5F).

Snail-Regulated Genes in Colonospheres

Although Snail induced various phenotypes, the underlying mechanisms are as yet unclear. We performed gene expression microarray analysis on SW480-Snail and SW480-Vector cells to gauge the transcriptome alternations induced by Snail. The gene expression patterns of these 2 cell lines were compared with those of various somatic or embryonic stem cells to assess any relationships present. Multidimensional scaling analysis showed that SW480-Snail cells were more similar to stem cells than SW480-Vector cells; mesenchymal stem cells and epithelial precursor cells were the closest cell types (Figure 4A). A dedifferentiated transcriptome drift is therefore induced by Snail in CRC cells.

In-depth analysis found that Snail regulated 3848 genes (Supplementary Table 3). Of those genes, 493 were also deregulated in colonospheres, with 227 being up-regulated and 266 being down-regulated in common (Figure 4B and Supplementary Table 4). Because increasing evidence shows that genes do not act individually but rather collaborate in genetic networks, we subjected the Snail up-regulated colonosphere genes to an interactome analysis. A single major network consisting of most of the known stemness-related or pro-proliferating genes was identified (Figure 4C). Within this network, CD44 is the CRC stem cell marker that we had previously identified. Furthermore, LIF, CCL20, IL8, CXCL2, CD44, PDGFB,

THBS1, and TNFRSF11B are secreted or cell membrane proteins and are therefore targetable by drugs (Figure 4C, in yellow). This network also revealed genes with significant biological roles in the CRC stem-like cells; namely, IL8, JUN, EGR1, and CCND1 are hubs that show very high connectivity to other genes (Figure 4C). Dysregulation of these hubs may eventually lead to the disruption of the genetic network and malfunctioning of the colonosphere cells. Six Snail-regulated genes from the array analysis, including IL8 and JUN, were confirmed by qPCR (Figure 4D). The level of IL8 expression was found to be correlated with Snail in the CRC cell lines and primary colonospheres (Figure 4E; correlation coefficient = 0.819 by Pearson correlation, $P = .004$). Of note, the Snail expression levels in the SW480-Snail stable cell line, the HCT15-Snail stable cell line, and the cell line-derived colonospheres were similar to those in the primary colonospheres (Supplementary Figure 6).

Coexpression of Snail, IL8, and CD44 in CRC Tissues

It has been reported that patients with CRC who have abundant Snail protein expression are more likely to develop distant metastases and have a poor survival outcome.^{8,9,22} Overexpression of IL8 also correlates with a poor CRC prognosis.²³ To investigate the correlation between Snail and IL8 levels in cancer tissues and whether the Snail/IL8 axis is associated with the putative tumor-initiating cell marker CD44, we initially investigated the expression levels of these 3 genes in the NCI-60 array data set.²⁴ Cells that had undergone EMT, based on a negative correlation between Snail and CDH1 (E-cadherin), were selected for this task. The IL8 and CD44 levels were positively correlated with Snail in CRC cells as well as in cells of other cancer types ($P = .001$ and $P = .002$, respectively; Figure 5A). Immunohistochemistry analysis was then performed on 52 paraffin-embedded CRC tissue samples (Supplementary Figure 7A). Two cases with triple-positive or triple-negative staining for Snail/IL8/CD44 are shown in Figure 5B. A significant correlation between Snail and IL8 ($P = .009$, Figure 5C) and between Snail and membranous CD44 ($P = .014$, Figure 5D) was found. In contrast, CD24 and CD133 expression levels did not correlate with Snail expression (Supplementary Figure 7B–D). IL8 was also correlated with CD44 expression ($P = .024$, Figure 5E). Furthermore, coexpression of Snail and IL8 showed a high correlation with the level of membranous CD44 ($P = .005$, Figure 5F). These results suggest the existence of a Snail/IL8 axis in clinical CRC samples and the correlation of this axis with the tumor-initiating cell marker CD44.

Direct Activation of IL8 Gene by Snail Through E-Boxes

Although Snail is a well-known transcription repressor,^{25,26} reports have also shown that Snail is able to activate gene expression directly.²⁷ We elucidated how Snail activates IL8 expression. Overexpressing Snail in

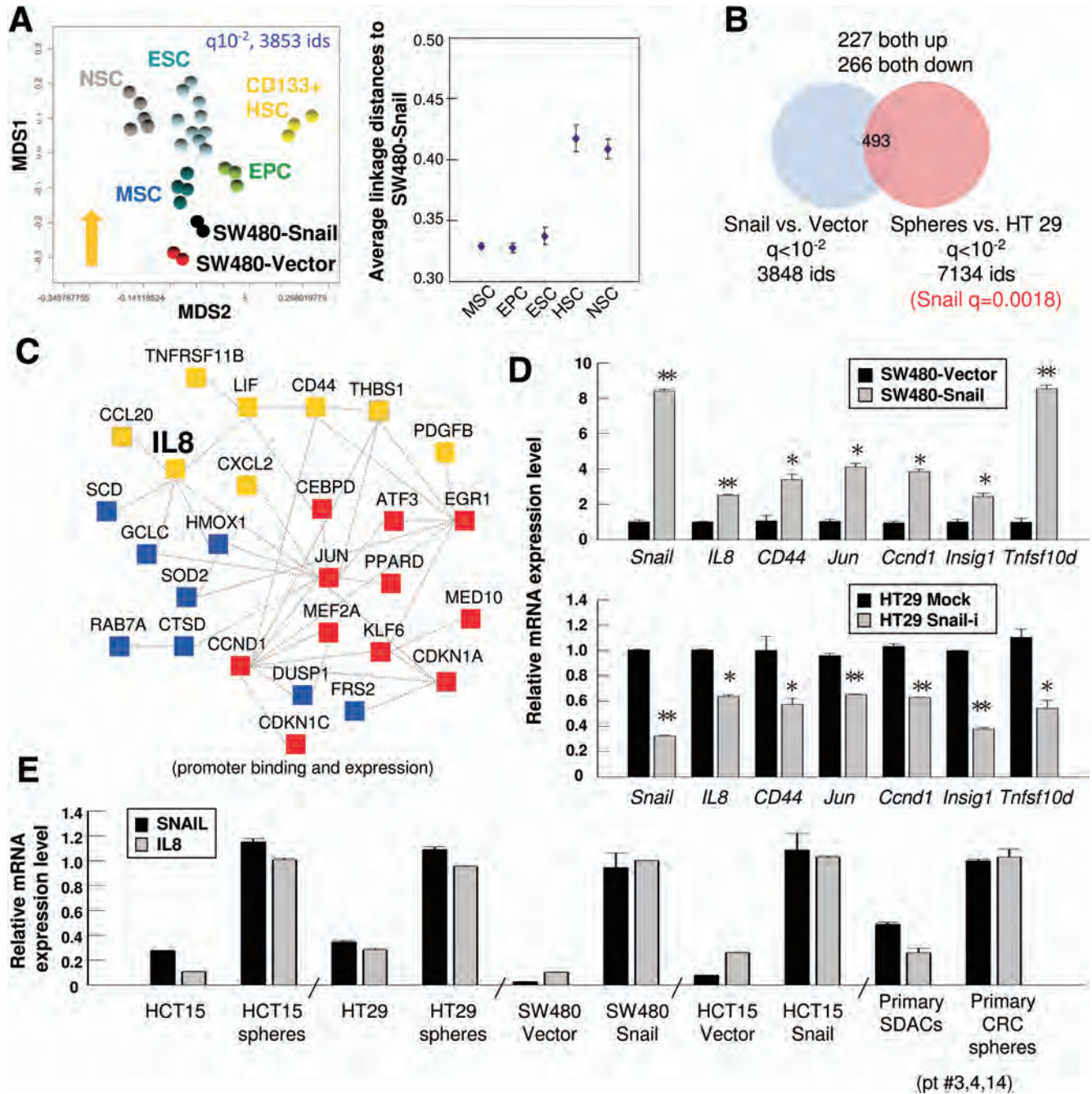


Figure 4. Systems biology analysis reveals various key Snail-regulated genes. (A) Dedifferentiation-like transcriptome alteration induced by Snail. A multidimensional scaling plot using Snail-regulated genes ($q < 10^{-2}$, 3848 probe sets). An arrow points out the transcriptome drifting direction (left). Transcriptome distance analysis for Snail-SW480 and various stem cells (right). (B) Venn diagram detailing shared distinct genes among Snail-regulated genes and colonosphere-specific genes. (C) A genetic network derived from 227 Snail up-regulated colonosphere genes. All have putative Snail-binding sites within their promoters. Yellow, secreted/membrane; blue, cytoplasmic; red, nuclear. (D) Reverse-transcription qPCR confirmation of genes modulated by Snail in SW480-Snail and Snail-depleted HT29 cells. * $P < .05$; ** $P < .01$. (E) Comparison of Snail and IL8 expression levels in CRC colonospheres, Snail ectopic-expressing cells, and corresponding control cells.

SW480 CRC cells induced cell motility, increased invasiveness (Figure 6A), and increased the IL8 protein level (Figure 6A). Ten putative Snail-binding sites, E-boxes with a motif sequence CANNTG, were identified in the proximal (-2000 to +100 base pairs) promoter region of *IL8*. This suggests that Snail may up-regulate *IL8* expression by binding directly to the *IL8* promoter. Chromatin immunoprecipitation assays identified the

presence of an interacting *IL8* promoter fragment containing the first 4 E-boxes in SW480-Snail cells (Figure 6B), HCT15-Snail cells, and colonospheres (Supplementary Figure 8A and B). A positive control band for the *CDH1* promoter region was also obtained as expected (Figure 6B and Supplementary Figure 8A and B, first row).

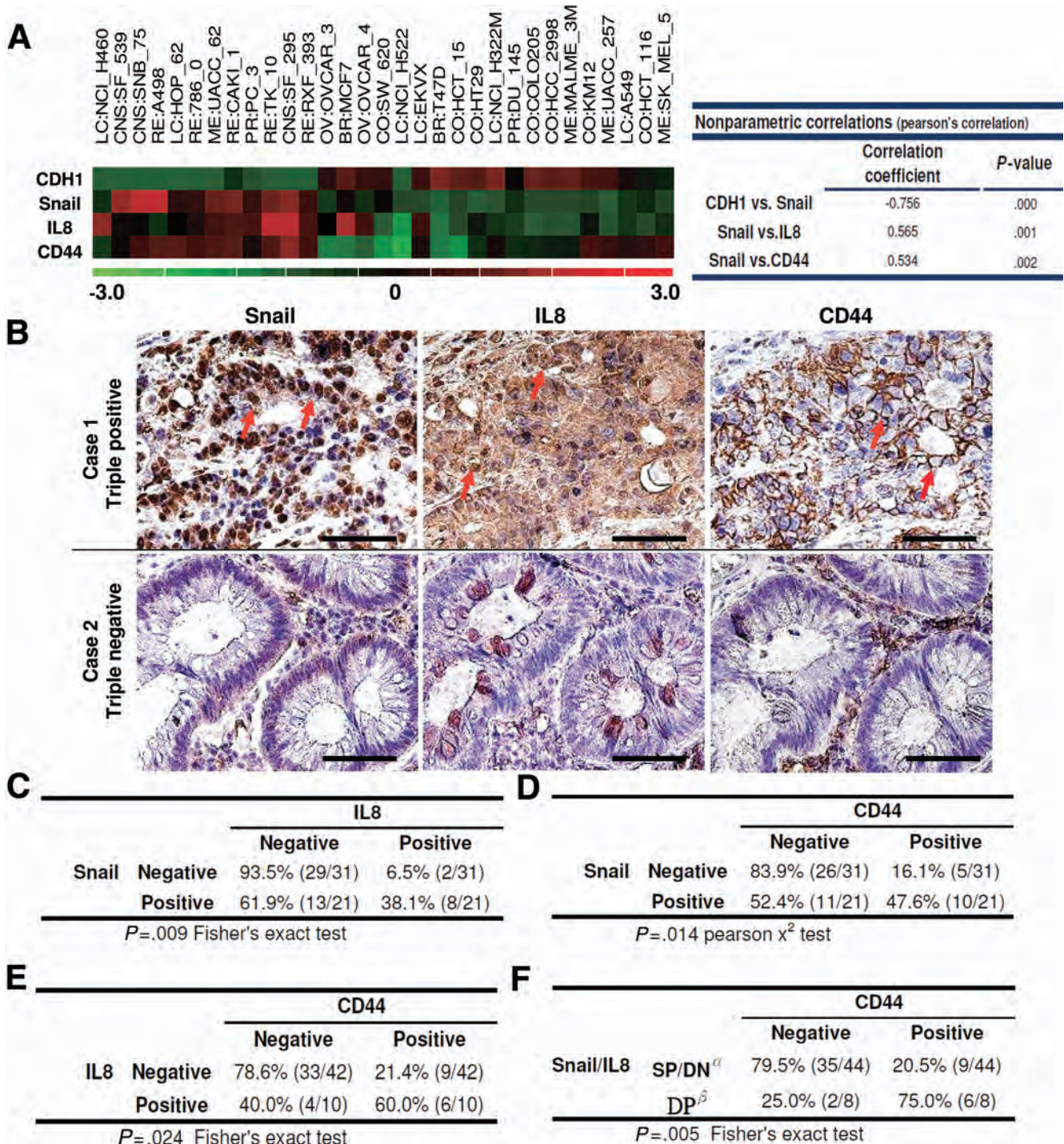
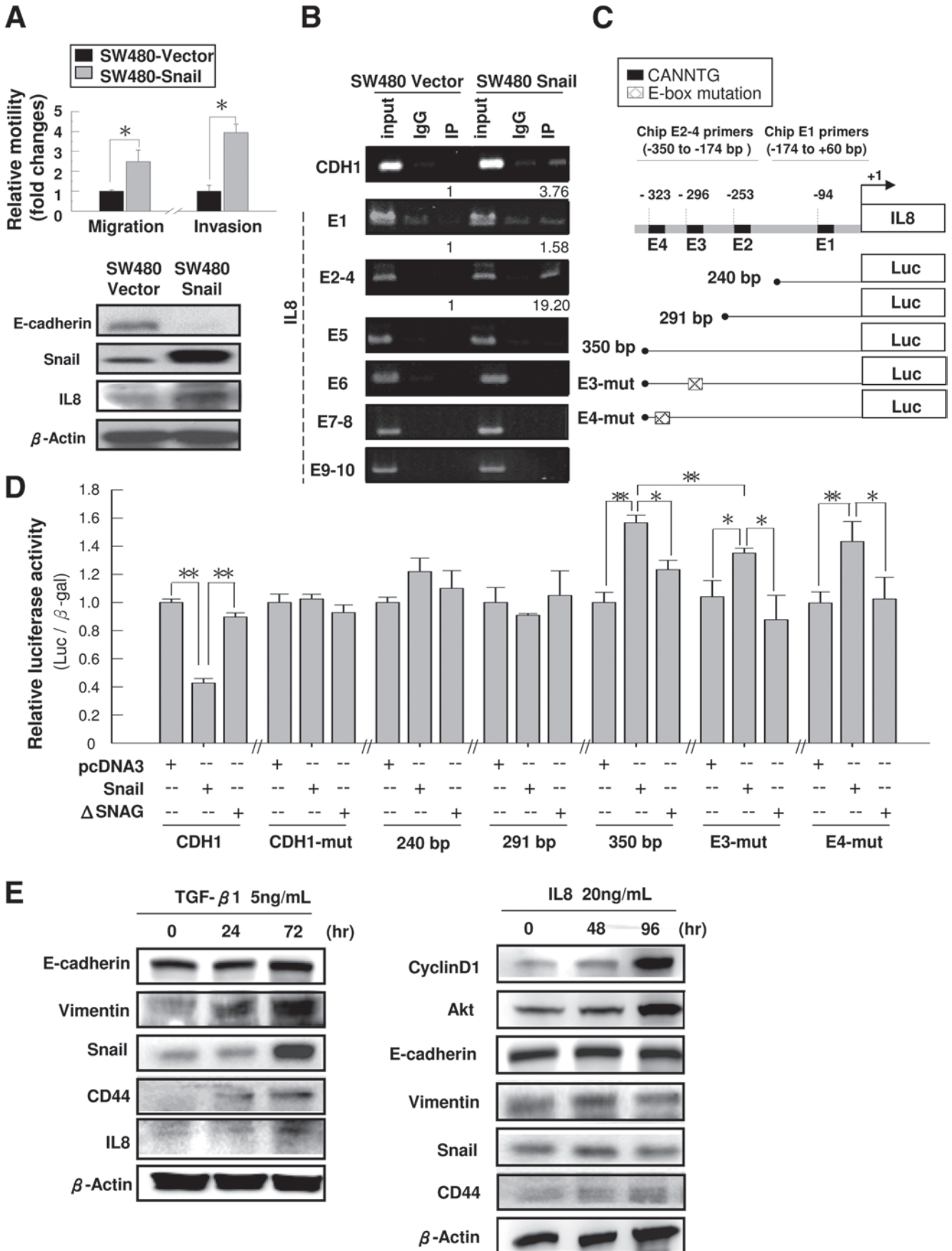


Figure 5. Snail positively correlates with IL8 and CD44 in NCI-60 cells and CRC tissues. (A) (Left) Heat map shows the relative expression level of CDH1, Snail, IL8, and CD44 from 31 selected NCI-60 cell lines. Genes in red, increased expression; in green, decreased expression. (Right) Pearson's correlation between Snail, IL8, and CD44 (correlation coefficient and *P* value). (B) Representative pictures of triple positive (upper row) and triple negative (lower) CRC cases. Scale bar = 100 μ m; red arrows, positively stained cells. (C–F) Statistical analysis of correlation between (C) Snail and IL8, (D) Snail and CD44, (E) IL8 and CD44, and (F) Snail/IL8 and CD44. α , single-positive or double-negative staining; β , double-positive staining.

Figure 6. Snail activates *IL8* transcription by binding directly to E-box motifs. (A) Relative migration and invasion abilities of SW480-Snail and SW480-Vector clones (upper). Immunoblotting of E-cadherin, Snail, and IL8 (lower). (B) Chromatin immunoprecipitation analysis with immunoglobulin G control or Snail-specific antibody. The 221–base pair (–194 to +27) product from the CDH1 proximal promoter was used as a positive control. Input: 2% total lysates. Fold chromatin enrichment indicated. (C) Schematic representation of *IL8* promoter region and reporter constructs. (D) Reporter activity of tested reporter plasmids after cotransfection with empty vector (pcDNA3), wild-type Snail (Snail), or SNAG deleted mutant (Δ SNAG). **P* < .05; ***P* < .01. (E) Immunoblotting analysis of transforming growth factor β 1-treated (left) and IL8-treated (right) HCT15 cells.



We next performed reporter assays to investigate whether the *IL8* promoter can be activated by Snail and to identify critical binding sites for Snail located within the *IL8* promoter. This was done using reporter constructs containing different lengths of the *IL8* promoter. Wild-type or mutated *CDH1* promoter-containing reporter constructs were used as controls (Figure 6C). An increase in *IL8* promoter activity was observed after transient transfection with wild-type Snail (Figure 6D, the “350 bp” group), while *CDH1* promoter activity was repressed (Figure 6D, *CDH1*). Transfection with an inactive Snail mutant (Snail[ΔSNAG])²⁸ neither activated the *IL8* promoter nor suppressed the *CDH1* promoter (Figure 6D). Deleting a region containing the putative E3 and E4 E-boxes (−352 to −291 base pairs) abolished *IL8* promoter activation (Figure 6D, 291 base pairs). Site-directed mutagenesis of the E3 or E4 E-box hampered activation, with modification of the E3 having a higher impact (Figure 6D). These results show that Snail activates the expression of *IL8* directly by binding to the E3/E4 E-boxes.

We next investigated whether IL8 is able to up-regulate Snail expression and form a feedback regulatory loop. When HCT15 cells were treated with recombinant IL8, although the positive controls using cyclin D1 and AKT were successfully induced,²⁹ neither Snail nor CD44 was up-regulated (Figure 6E). In contrast, transforming growth factor β 1 successfully induced Snail expression and EMT in the same batch of cells (Figure 6E).

IL8 Is Critical for Snail-Induced Stemness and Targeting IL8 Inhibits CRC Tumor Growth

To show whether IL8 is required for the various Snail-induced phenotypes, small hairpin RNA-mediated *IL8* repression was performed in SW480-Snail, HCT15-Snail, and HT29 cells. Stably down-regulating IL8 resulted in decreased expression of stemness genes (including *Sox2*, *Nanog*, and *Oct4*; Figure 7A and Supplementary Figure 9A). Neutralizing IL8 activity by IL8 neutralizing antibody (nAb) in primary, HT29, and HCT15 colonospheres also affected the expression of *Sox2*, *Nanog*, or *Oct4* (Figure 7A, right panel, Supplementary Figure 9A, right panel, and Supplementary Figure 9B). Knocking down of IL8 in cells overexpressing Snail or treating colonospheres with IL8 nAb diminished both first and second sphere formation (Figure 7B and C and Supplementary Figure 9C and D). The chemoresistance of SW480-Snail, HCT15-Snail, and HT29 cells was reduced when *IL8* expression was blocked (Figure 7D and Supplementary Figure 9E). Furthermore, treating HT29 and HCT15 colonospheres with IL8 nAb sensitized them to the conventional chemotherapy drug 5-fluorouracil in a dose-dependent manner (Figure 7D, right panel, and data not shown).

IL8 is a well-known angiogenic chemokine.³⁰ Induction of angiogenic phenotypes by selecting colonospheres or by Snail overexpression is able to be abolished by inactivation of IL8, as shown by endothelial cell proliferation, migration, and tube formation assays (Supplementary Figure 10). In vivo implantation assays showed that stable

knockdown of *IL8* expression in SW480-Snail or HT29 colonosphere cells before implantation significantly decreased tumor size (Supplementary Figure 11). When IL8 nAb was repeatedly injected into existing CRC bulky tumors, a significant reduction in the growth of the xenografts was observed (Figure 7E). As expected, IL8 nAb also resulted in the down-regulation of Oct4 and Sox2 expression in vivo (Figure 7F).

Discussion

Tumor development, progression, and prognosis remain positioned at the front line of medical research. Clinically, cancer cells with a poor differentiated pathological grading usually have a worse therapy response.¹ It has been proved that *c-Myc*, but not other tested oncogenes, is sufficient to reactivate the embryonic stem cell-like program in normal and cancer cells.³¹ The convergence of dedifferentiation and cancer malignancy also came from the discovery that EMT or Snail overexpression can induce the formation of mammospheres from transformed breast cancer epithelial cells and that tumor stem cells that have undergone EMT are more motile and show greater metastatic ability.^{3,4} However, it is still unclear how Snail contributes to cell dedifferentiation. We found that IL8 is a direct downstream target of Snail and that the Snail/IL8 axis seems to play a critical role in CRC stemness and malignancy. This discovery holds the promise of resolving major problems when treating colon cancer and other EMT-related phenomena because EMT regulators are not available as therapeutic drug targets at present.

Increased expression of the proangiogenic/proinflammatory chemokine IL8 (CXCL8) and/or its receptors (CXCR1/CXCR2) has been characterized in various cancer cells, endothelial cells, infiltrating neutrophils, and tumor-associated macrophages, which suggests that IL8 may function as a significant regulatory factor within the tumor microenvironment.³⁰ In prostate cancer, IL8 is a molecular determinant of androgen-independent cancer growth and progression.^{30,32} In colon cancer, IL8 is up-regulated in cancerous tissues and is associated with tumor progression, liver metastasis, and poor tumor differentiation.^{23,33} IL8 also significantly stimulates the proliferation, migration, and invasion of CRC cells.^{33,34} A very recent report has shown that IL8 is able to be up-regulated by deoxycholic acid in *adenomatous polyposis coli* (*APC*) gene-deficient cells during the initiation of colonic epithelium and that neutralizing IL8 is able to reduce the invasive potential of tumors.³⁵ IL8 has been linked to EMT in cancers because during transforming growth factor β -initiated EMT, IL8, and CXCR1 expression is induced.³⁶ Induction of IL8 also preserves the angiogenic response in HIF1 α -deficient CRC cells.³⁷ Because Snail is induced by hypoxia and transforming growth factor β ,³⁸ the previously described findings hint at a link between IL8 and Snail. In this study, we have proven that there is a direct and causal connection between IL8 and Snail

discover new anticancer drugs. Agents targeting various oncogenic pathways in colon cancer have been developed and tested in clinical trials.⁴¹ Various relationships between cytokines/chemokines and cancer stem cells have also recently been noticed. IL6 signaling has recently been shown to make a significant contribution in glioma stem cells.⁴² Treating glioma stem cells with IL6 antibody decreases subcutaneous xenograft growth in mice.⁴² IL6, together with IL17, also makes a contribution to tumor-like stem cells derived from human keloid.⁴³ We found that HT29 cancer stem-like cells also express more IL1 β , IL32, CCL28, CCL20, CCL14, and CXCL1–3 when compared with parental HT29 cells (Supplementary Table 2). CXCL2 and CCL20 are also up-regulated by Snail and enriched in colonospheres (Figure 4C). A combined therapy using an antibody cocktail thus may improve therapeutic effects on patients with CRC.

CD44⁺ cells, as well as CD133⁺, CD24⁺, and CD166⁺ cells, were enriched in colonospheres derived from either clinical tissues or cell lines (Figure 1A). Such complexity may reflect the heterogeneity of the cancer stem cell population in colon cancer. Whether all CD44⁺ cells are cancer stem cells remain to be seen. Nevertheless, the CD44⁺ population is consistently enriched in colonospheres (Figure 1A), and CD44⁺ cells sorted from colonospheres were found to be more malignant than CD44⁻ cells (Supplementary Figure 12). CD44 expression would seem to be induced by Snail (Figure 3C and Supplementary Figure 5C) and was found to correlate with Snail and IL8 expression (Figure 5D and E). The Snail-IL8 axis therefore plays a crucial role in the CD44⁺ CRC/cancer stem cells subgroup to some extent.

Supplementary Material

Note: To access the supplementary material accompanying this article visit the online version of *Gastroenterology* at www.gastrojournal.org and at 10.1053/j.gastro.2011.04.008.

References

- Ben-Porath I, Thomson MW, Carey VJ, et al. An embryonic stem cell-like gene expression signature in poorly differentiated aggressive human tumors. *Nat Genet* 2008;40:499–507.
- Yang MH, Wu KJ. TWIST activation by hypoxia inducible factor-1 (HIF-1): implications in metastasis and development. *Cell Cycle* 2008;7:2090–2096.
- Mani SA, Guo W, Liao MJ, et al. The epithelial-mesenchymal transition generates cells with properties of stem cells. *Cell* 2008;133:704–715.
- Morel AP, Lievre M, Thomas C, et al. Generation of breast cancer stem cells through epithelial-mesenchymal transition. *PLoS ONE* 2008;3:e2888.
- Peinado H, Olmeda D, Cano A. Snail, Zeb and bHLH factors in tumour progression: an alliance against the epithelial phenotype? *Nat Rev Cancer* 2007;7:415–428.
- Medici D, Hay ED, Olsen BR. Snail and Slug promote epithelial-mesenchymal transition through beta-catenin-T-cell factor-4-dependent expression of transforming growth factor-beta3. *Mol Biol Cell* 2008;19:4875–4887.
- Backlund MG, Mann JR, Holla VR, et al. Repression of 15-hydroxyprostaglandin dehydrogenase involves histone deacetylase 2 and snail in colorectal cancer. *Cancer Res* 2008;68:9331–9337.
- Palmer HG, Larriba MJ, Garcia JM, et al. The transcription factor SNAIL represses vitamin D receptor expression and responsiveness in human colon cancer. *Nat Med* 2004;10:917–919.
- Pena C, Garcia JM, Silva J, et al. E-cadherin and vitamin D receptor regulation by SNAIL and ZEB1 in colon cancer: clinicopathological correlations. *Hum Mol Genet* 2005;14:3361–3370.
- Huber MA, Kraut N, Beug H. Molecular requirements for epithelial-mesenchymal transition during tumor progression. *Curr Opin Cell Biol* 2005;17:548–558.
- Dalerba P, Dylla SJ, Park IK, et al. Phenotypic characterization of human colorectal cancer stem cells. *Proc Natl Acad Sci U S A* 2007;104:10158–10163.
- Chen YC, Hsu HS, Chen YW, et al. Oct-4 expression maintained cancer stem-like properties in lung cancer-derived CD133-positive cells. *PLoS One* 2008;3:e2637.
- Todaro M, Alea MP, Di Stefano AB, et al. Colon cancer stem cells dictate tumor growth and resist cell death by production of interleukin-4. *Cell Stem Cell* 2007;1:389–402.
- Singh SK, Hawkins C, Clarke ID, et al. Identification of human brain tumour initiating cells. *Nature* 2004;432:396–401.
- Ieta K, Tanaka F, Haraguchi N, et al. Biological and genetic characteristics of tumor-initiating cells in colon cancer. *Ann Surg Oncol* 2008;15:638–648.
- Lombardo Y, Scopelliti A, Cammareri P, et al. Bone morphogenetic protein 4 induces differentiation of colorectal cancer stem cells and increases their response to chemotherapy in mice. *Gastroenterology* 2011;140:297–309.
- Lee J, Kotliarova S, Kotliarov Y, et al. Tumor stem cells derived from glioblastomas cultured in bFGF and EGF more closely mirror the phenotype and genotype of primary tumors than do serum-cultured cell lines. *Cancer Cell* 2006;9:391–403.
- Heath JK, White SJ, Johnstone CN, et al. The human A33 antigen is a transmembrane glycoprotein and a novel member of the immunoglobulin superfamily. *Proc Natl Acad Sci U S A* 1997;94:469–474.
- Johnstone CN, White SJ, Tebbutt NC, et al. Analysis of the regulation of the A33 antigen gene reveals intestine-specific mechanisms of gene expression. *J Biol Chem* 2002;277:34531–34539.
- Todaro M, Francipane MG, Medema JP, et al. Colon cancer stem cells: promise of targeted therapy. *Gastroenterology* 2010;138:2151–2162.
- Harris MA, Clark J, Ireland A, et al. The Gene Ontology (GO) database and informatics resource. *Nucleic Acids Res* 2004;32:D258–D261.
- Roy HK, Smyrk TC, Koetsier J, et al. The transcriptional repressor SNAIL is overexpressed in human colon cancer. *Dig Dis Sci* 2005;50:42–46.
- Rubie C, Frick VO, Pfeil S, et al. Correlation of IL-8 with induction, progression and metastatic potential of colorectal cancer. *World J Gastroenterol* 2007;13:4996–5002.
- Shoemaker RH. The NCI60 human tumour cell line anticancer drug screen. *Nat Rev Cancer* 2006;6:813–823.
- Cano A, Perez-Moreno MA, Rodrigo I, et al. The transcription factor snail controls epithelial-mesenchymal transitions by repressing E-cadherin expression. *Nat Cell Biol* 2000;2:76–83.
- Battle E, Sancho E, Franci C, et al. The transcription factor snail is a repressor of E-cadherin gene expression in epithelial tumour cells. *Nat Cell Biol* 2000;2:84–89.
- Lan L, Han H, Zuo H, et al. Upregulation of myosin Va by Snail is involved in cancer cell migration and metastasis. *Int J Cancer* 2010;126:53–64.
- Peinado H, Ballestar E, Esteller M, et al. Snail mediates E-cadherin repression by the recruitment of the Sin3A/histone deacetylase 1 (HDAC1)/HDAC2 complex. *Mol Cell Biol* 2004;24:306–319.

29. MacManus CF, Pettigrew J, Seaton A, et al. Interleukin-8 signaling promotes translational regulation of cyclin D in androgen-independent prostate cancer cells. *Mol Cancer Res* 2007;5:737–748.
30. Waugh DJ, Wilson C. The interleukin-8 pathway in cancer. *Clin Cancer Res* 2008;14:6735–6741.
31. Wong DJ, Liu H, Ridky TW, et al. Module map of stem cell genes guides creation of epithelial cancer stem cells. *Cell Stem Cell* 2008;2:333–344.
32. Araki S, Omori Y, Lyn D, et al. Interleukin-8 is a molecular determinant of androgen independence and progression in prostate cancer. *Cancer Res* 2007;67:6854–6862.
33. Cacev T, Radosevic S, Krizanac S, et al. Influence of interleukin-8 and interleukin-10 on sporadic colon cancer development and progression. *Carcinogenesis* 2008;29:1572–1580.
34. Itoh Y, Joh T, Tanida S, et al. IL-8 promotes cell proliferation and migration through metalloproteinase-cleavage proHB-EGF in human colon carcinoma cells. *Cytokine* 2005;29:275–282.
35. Rial NS, Lazennec G, Prasad AR, et al. Regulation of deoxycholate induction of CXCL8 by the adenomatous polyposis coli gene in colorectal cancer. *Int J Cancer* 2009;124:2270–2280.
36. Bates RC, DeLeo MJ III, Mercurio AM. The epithelial-mesenchymal transition of colon carcinoma involves expression of IL-8 and CXCR-1-mediated chemotaxis. *Exp Cell Res* 2004;299:315–324.
37. Mizukami Y, Jo WS, Duerr EM, et al. Induction of interleukin-8 preserves the angiogenic response in HIF-1 α -deficient colon cancer cells. *Nat Med* 2005;11:992–997.
38. Yang MH, Wu MZ, Chiou SH, et al. Direct regulation of TWIST by HIF-1 α promotes metastasis. *Nat Cell Biol* 2008;10:295–305.
39. Mian BM, Dinney CP, Bermejo CE, et al. Fully human anti-interleukin 8 antibody inhibits tumor growth in orthotopic bladder cancer xenografts via down-regulation of matrix metalloproteases and nuclear factor-kappaB. *Clin Cancer Res* 2003;9:3167–3175.
40. Bao Z, Ye Q, Gong W, et al. Humanized monoclonal antibody against the chemokine CXCL-8 (IL-8) effectively prevents acute lung injury. *Int Immunopharmacol* 2010;10:259–263.
41. Zhou BB, Zhang H, Damelin M, et al. Tumour-initiating cells: challenges and opportunities for anticancer drug discovery. *Nat Rev Drug Discov* 2009;8:806–823.
42. Wang H, Lathia JD, Wu Q, et al. Targeting interleukin 6 signaling suppresses glioma stem cell survival and tumor growth. *Stem Cells* 2009;27:2393–2404.
43. Zhang Q, Yamaza T, Kelly AP, et al. Tumor-like stem cells derived from human keloid are governed by the inflammatory niche driven by IL-17/IL-6 axis. *PLoS ONE* 2009;4:e7798.

Received January 15, 2010. Accepted April 1, 2011.

Reprint requests

Address requests for reprints to: Hsei-Wei Wang, PhD, Institute of Microbiology and Immunology, National Yang-Ming University, No. 155, Sec. 2, Li-nong Street, Taipei, 112 Taiwan; e-mail: hwwang@ym.edu.tw; fax: (886) 2-28212880 or Shih-Hwa Chiou, MD, PhD, Institute of Clinical Medicine, National Yang-Ming University, No. 155, Sec. 2, Li-nong Street, Taipei, 112 Taiwan; e-mail: shchiou@vghtpe.gov.tw; fax: (886) 2-28745074.

Acknowledgments

The authors thank the Microarray & Gene Expression Analysis Core Facility of the National Yang-Ming University VGH Genome Research Center for their technical support. The shRNA plasmids were provided by the National RNAi Core Facility, Taiwan.

Array data produced in this work are available from the GEO database (accession no. GSE14773).

Writing assistance for this manuscript was provided by Prof Ralph Kirby under the support of Yang-Ming University (a grant from Ministry of Education, Aim for the Top University Plan) and Taipei Veterans General Hospital Research Fund, VGHUST Joint Research Program, Tsou's Foundation (VGHUST99-P6-31).

W.-L.H. and M.-H.Y. contributed equally to this work.

Conflicts of interest

The authors disclose no conflicts.

Funding

Supported by Yang-Ming University (a grant from Ministry of Education, Aim for the Top University Plan), Taipei Veterans General Hospital (V97ER2-001, V98ER2-003 and DOH100-TD-C-111-007, Center of Excellence for Cancer Research at Taipei Veterans General Hospital), Taipei Veterans General Hospital Research Fund, VGHUST Joint Research Program, Tsou's Foundation (VGHUST99-P6-31), Taipei City Hospital (99001-62-012), and partly by NSC (NSC97-3112-B-010-007, NSC98-3111-B-010-004 and NSC97-3111-B-075-001-MY3).

Supplementary Materials and Methods

Cell Culture

Cell lines including human CRC lines (SW480 and HT29), human medulloblastoma HTB-186 (a DAOY metastatic cell line), and embryonic kidney 293T cells were grown in Dulbecco's modified Eagle medium (DMEM; Gibco, Carlsbad, CA) supplemented with 10% fetal bovine serum (FBS; Gibco). Human CRC lines HCT15 and SW620 and hypopharyngeal carcinoma FaDu cells were grown in RPMI 1640 (Gibco) supplemented with 10% FBS. Human CRC cell LS174T was grown in Eagle's MEM (Gibco) supplemented with 10% FBS (Gibco) and 1% NEAA (Gibco). Immortalized human microvascular endothelial cells HMEC-1 (ATCC no. CRL 10636) were cultured in endothelial cell growth medium MV (EGM MV; PromoCell, Heidelberg, Germany), and human umbilical vein endothelial cells were cultured in EGM MV-2 (PromoCell) medium on fibronectin-coated (Sigma, St Louis, MO) dishes.

Spheroid Formation and Anchorage-Independent Colony Formation Assay

Parental cells and colonospheres were dissociated into single-cell suspension by TrypLE Express (Invitrogen, Carlsbad, CA). A total of 1000 or 10,000 (for SW480) cells were suspended in stem cell medium by limiting dilution and cultured in a well of 96-well plates for 15 days. Spheroids larger than 50 μm were counted, and colonospheres formed per well were considered as the spheroid-forming index. More than 20 wells were counted in each experimental set. In IL8-depleted spheroid formation experiments, 1 to 20 $\mu\text{g}/\text{mL}$ IL8 nAb (catalog no. AF-208-NA; R&D Systems Inc, Minneapolis, MN) or 20 $\mu\text{g}/\text{mL}$ normal goat immunoglobulin (Ig) G control (catalog no. AB-108-C; R&D Systems Inc) was added and fresh nAbs were supplemented again after 1 week. Anchorage-independent colony formation assay was performed as follows: each well (35 mm) of a 6-well culture dish was coated with 1 mL bottom agar mixture (RPMI or DMEM, 15% [vol/vol] FBS, 0.5% [wt/vol] agar, 1% [vol/vol] penicillin-streptomycin). After the bottom layer was solidified, 1 mL of top agar-medium mixture (RPMI or DMEM, 15% [vol/vol] FBS, 0.3% [wt/vol] agar, 1% [vol/vol] penicillin-streptomycin) containing 5000 cells was added, and the dishes were incubated at 37°C for 2 to 4 weeks. Plates were stained with 0.5 mL of 0.005% crystal violet for 1 hour before counting colony numbers.¹

In Vivo Metastasis Assay, Tumorigenicity Assay, and Green Fluorescence Intensity Detection

All procedures involving animals were in accordance with the Institutional Animal Welfare Guidelines of the Taipei Veterans General Hospital. BALB/c nude mice or NOD/SCID mice were purchased from the Na-

tional Laboratory Animal Center, Taiwan, and were bred and maintained according to the Guidelines for Laboratory Animals in the Taipei Veterans General Hospital. Metastatic capability was determined by injected identical numbers of HT29-green fluorescent protein (GFP) parental and dissociated HT29-GFP colonosphere cells into the subcapsular region of spleen in anesthetized BALB/c nude mice. Mice were killed and examined for organ metastasis 3 months after injection. Tumorigenicity was determined by subcutaneously injecting parental cells, sorted cells, dissociated colonospheres, or stable cell lines into flanks of 6- to 8-week-old BALB/c nude mice (for HT29 and SW480 cells) or NOD/SCID mice (for HT29 and HCT15 cells). In IL8-depleted tumorigenic assay, 2 μg IL8 nAb (catalog no. AF-208-NA; R&D Systems) and normal goat IgG control (catalog no. AB-108-C; R&D Systems Inc) were injected into the preestablished, HT29 colonosphere-derived tumor twice a week for a month (tumor volume reached about 50 mm^3). Tumor sizes were measured with calipers, and tumor volumes were calculated according to the following formula: $(\text{Length} \times \text{Width}^2)/2$. In vivo GFP imaging was visualized and measured by an illuminating device (LT-9500 Illumatool TLS [Lighttools Research, Encinitas, CA] equipped with excitation illuminating source [470 nm] and filter plate [515 nm]). The integrated optical density of green fluorescence intensity was captured and then analyzed by Image Pro-plus software (Media Cybernetics, Silver Spring, MD).²⁻⁴

Array Data and Bioinformatics Analysis

Total RNA was extracted for Affymetrix Human Genome U133 Plus 2.0 Array (Affymetrix, Santa Clara, CA) analysis. RNA collection, array hybridization, and feature selection were performed as described.⁵ Stem cell array data were described in our previous work,⁶ and epithelial precursor cell (EPC) array data were downloaded from the ArrayExpress database (E-MEXP-993).⁷ Gene expression array data of the NCI-60 cell lines implemented with Affymetrix HG-U133A and U133B chip platforms were downloaded from the CellMiner database (<http://discover.nci.nih.gov/cellminer/>).⁸ Genetic network construction was performed by the Pathway Studio 6.2 (Ariadne Genomics, Rockville, MD) and the Ingenuity Pathway Analysis (IPA) software (Ingenuity Systems, Redwood City, CA). Heat maps were created using dChip software (<http://biosun1.harvard.edu/complab/dchip/>). Classical multidimensional scaling was performed using the standard function of the R program to provide a visual impression of how the various sample groups are related. The average-linkage distance was used to assess the similarity between 2 groups of gene expression profiles as described.⁵ The difference in distance between 2 groups of sample expression profiles to a third was assessed by the comparison of corresponding average linkage distances (the mean of all pairwise distances [link-

ages] between members of the 2 groups concerned). The error on such a comparison was estimated by combining the standard errors (the standard deviation of pairwise linkages divided by the square root of the number of linkages) of the average-linkage distances involved.⁵ Gene annotation was performed by the ArrayFusion web tool (<http://microarray.yu.edu.tw/tools/arrayfusion/>)⁹ and gene enrichment analysis by the DAVID 2008 Bioinformatics Resources (<http://david.abcc.ncifcrf.gov/>).¹⁰

Reverse Transcription and Reverse-Transcription qPCR

One microgram of total RNA was subjected into first-strand complementary DNA synthesis by using the SuperScript III Reverse Transcriptase Kit (Invitrogen) as directed by the manufacturer. To design PCR primers, human pre-messenger RNA sequences were obtained from the National Center for Biotechnology Information AceView program (www.ncbi.nlm.nih.gov/AceView/) and all primers were designed by the Primer Express software (Applied Biosystems, Carlsbad, CA). All the primer sequences are listed in Supplementary Table 5A.

Reverse-transcription qPCR reactions were performed to validate expression level by using SYBR Green Supermix (BioRad, Hercules, CA), and specific products were detected and analyzed using the Roche LC480 real-time system (Roche, Basel, Switzerland). The expression level of each gene was normalized to the endogenous expression level of GAPDH and experimental control through $\Delta\Delta C_t$ methods.

Transient Transfection, Reporter Assay, and Chromatin Immunoprecipitation

Lipofectamine 2000 (Invitrogen) reagent was used for establishing stable lines (SW480-Snail, HCT15-Snail, and their corresponding vector controls), for transient transfection in Snail small hairpin RNA (shRNA) targeting experiment, and for reporter assays. The IL8 promoter region (-350 to +16 base pairs) was cloned by PCR amplification of genomic DNA from 293T cells and then inserted into the *Bgl*II/*Hind*III sites of the pXP2 vector to generate the pXP2-IL8-350 parental construct. Various lengths of promoter fragments and E-box mutated fragments were cloned by PCR amplification of pXP2-IL8-350 parental construct into the pXP2 vector (Figure 6C). CDH1 reporter³ and CDH1-mut reporter that contained mutated E-box were used as experimental controls. Reporter constructs were cotransfected with indicated expression constructs (Figure 6D) and β -gal internal control plasmids into 293T for 48 hours before the luciferase activity was measured.² All primers used in reporter construction are listed in Supplementary Table 5C. For chromatin immunoprecipitation assay, chromosomal DNA fragments were prepared as described.² Briefly, lysates were incubated with isotype IgG (catalog no. sc-2027;

Santa Cruz Biotechnology Inc, Santa Cruz, CA) or antibody specific for Snail (catalog no. ab17732; Abcam, Cambridge, MA). The 221-base pair product from CDH1 proximal promoter (-194 to +27 base pairs) flanking the -25/-80 E-box was used as a positive control. The primers used in chromatin immunoprecipitation assays are listed in Supplementary Table 5B.

Drug Resistance and MTT Assay

A total of 1×10^4 cells were seeded per well in a 96-well plate and incubated overnight before treating with various concentrations of drugs. After 48 hours, medium was discarded and MTT assay solution was added onto cells for 3 hours at 37°C. Newly formed mitochondrial MTT crystals were dissolved with DMSO (J.T. Baker, Phillipsburg, NJ) and then read by a microplate reader (OD560/670; Spectramax 250, Molecular Devices Corp, Minneapolis, MN). To examine the drug resistance ability of IL8-depleted cells, 3 to 20 μ g/mL IL8 nAb (catalog no. AF-208-NA; R&D Systems Inc) or 20 μ g/mL normal goat IgG control (catalog no. AB-108-C; R&D Systems Inc) was pretreated for 12 hours on cells. These cells were then treated with drugs in the presence of nAb for another 48 hours.

Radiation Resistance Assay and Survival Curve

The radiation resistance assay was performed as described.⁴ Briefly, 500 cells were seeded in RPMI 1640 (Gibco) supplemented with 10% FBS in a T25 flask 16 hours before Co-60 irradiation. Gamma radiation was delivered by Theratron cobalt unit T-1000 (Theratron International, Inc, Ottawa, Canada) at a dose rate of 1.1 Gy/min (SSD = 57.5 cm). Each flask was exposed to 0, 2, 4, 6, 8, or 10 Gy radiation intensity of Cobalt-60 under the guidance of Taipei Veterans General Hospital, and colonies were stained with Giemsa stain at day 14 after radiation exposure. The survival curve was composed of survival fraction versus different radiation doses. The survival fraction was calculated by the following formulas: SF = Number of Colonies/Plating Cells \times PE. PE (Plating Efficiency) = Numbers of Control Colonies/Seeding Cell Numbers.

Plasmid, siRNA, and shRNA Clones

pcDNA3.1-Snail construct, pcDNA3.1 vector, pSUPER-scramble-siRNA, pXP2 reporter vector, and CDH1(E-cadherin) reporter were from a previous work.³ The pSUPER-Snail-siRNA construct was generated previously.¹¹ The SNAG domain-deleted Snail mutant (Snail-[SNAG]),¹² CDH1-mut reporter containing mutated E-box, and all the constructions mentioned previously were kindly provided by Dr M-H Yang. Various lengths of IL8 promoter fragments and fragments containing mutated E-box were inserted upstream of the luciferase gene from *Bgl*II to *Hind*III sites in the pXP2 vector (ATCC no.

37577). The reporter fragments E3-mut and E4-mut were generated by SOE PCR (splicing by overlap extension PCR) containing one mutated sequence in which the E-box (CANNTG) sequence was mutated from CACATG to TGTGCA and from CACCTG to TGTTCA, respectively (Figure 6C).

Lipofectamine 2000 (Invitrogen) reagent was used for stable line establishment and for transient transfection in reporter assays. To transiently silence the expression of endogenous target genes, Snail-specific small interfering RNA (siRNA) duplex (5-GCGAGCUGCAGGACUC-UAAAdTdT-3)¹³ was synthesized (Sigma). The DharmaFect #4 transfection reagent (Dharmacon RNAi Technologies, Chicago, IL) or Lipofectamine 2000 (Invitrogen) reagent was applied for siRNA gene silencing experiments in HT29 parental cells following the manufacturer's instructions. To stably knock down IL8 expression in HT29 parental cells, HT29 colonospheres, and SW480-Snail and HCT15-Snail stable cell lines, 4 IL8 shRNA constructs (TRCN0000058028-31) targeting the 3'UTR and CDS region of IL8 transcript were obtained from the National RNAi Core Facility (<http://rna.genmed.sinica.edu.tw/>) for lentivirus-based gene silencing. A shRNA vector against luciferase (pLKO.1-shLuc) was used as a negative control. A pCDH1-MCS1-EF1-CopGFP vector (Systems Biosciences, Mountain View, CA) was used as a transduction control during lentivirus infection. All constructs were verified by sequencing.

Lentivirus Production and Transduction

For virus package, pCMV Δ R8.7, pDVsVg (from the National RNAi Core Facility, Taiwan), and pCDH1-MCS1-EF1-CopGFP were cotransfected into 293T cells by Lipofectamine 2000 (Invitrogen). Forty-eight to 72 hours later, virus supernatant was harvested for concentration. For virus transduction, cells were seeded onto 6-cm dishes and infected with 20-fold virus concentrates supplemented with 8 μ g/mL Polybrene (catalog no. 9268; Sigma, St. Louis, MO) for 12 hours before replacing with fresh medium. Cells were then selected by GFP sorting or puromycin (Sigma) for 2 weeks.

Immunohistochemistry Staining and Immunoblotting

Tumor specimens from mice or clinical human patients were washed with 1 \times phosphate-buffered saline (PBS), fixed with 4% paraformaldehyde (Sigma), and embedded in Parafilm. All procedures were approved by the Institutional Review Board at the Taipei City Hospital, Taiwan. Sections (4 μ m thick) were deparaffinized and rehydrated before staining. Tissue antigens were retrieved by boiling in 10 mmol/L (pH 6) citrate buffer (Sigma) 3 minutes for 6 times. Sections were cooled down on ice for 30 minutes before treating with 3% H₂O₂. Samples were permeabilized in 0.2%

Triton X-100 (X-878; Sigma) in PBS and blocked in 5 mg/mL BSA (V-964; Sigma) in PBS for 30 minutes before hybridizing with 200 \times diluted primary antibodies Snail (catalog no. ab17732; Abcam), IL8 (catalog no. AF-208-NA; R&D Systems Inc), CD44 (catalog no. 3570; Cell Signaling, Beverly, MA), CD133 (catalog no. 3663S; Cell Signaling), and CD24 (catalog no. MAB5248; R&D Systems Inc) overnight at 4°C. Sections were then stained with 200 \times diluted secondary antibodies (catalog no. sc-2370, sc-2954, and sc-2953; Santa Cruz Biotechnology, Santa Cruz, CA) for 30 minutes at room temperature. Signals were amplified by the TSA Biotin System (PerkinElmer, Waltham, MA) as instructed by the manufacturer and then counterstained with hematoxylin QS (H-3404; Vector Laboratories, Burlingame, CA) for 20 seconds. For immunohistochemistry grading, the immunoreactivity of Snail was scored as follows: 0, no nuclear staining; 1+, weak nuclear staining; and 2+, strong nuclear staining. Only 2+ was interpreted as increased Snail expression (Supplementary Figure 7A I-III). IL8 expression was scored as follows: 0, no cytoplasmic expression; 1+, weak cytoplasmic staining; and 2+, strong cytoplasmic staining. Only 2+ was considered as increased IL8 expression (Supplementary Figure 7A IV-VI). For CD44 expression, we graded the samples into negative when <5% of membranous CD44 was detected in cancer cells, whereas positive cases indicated \geq 5% of cancer cells had membranous CD44 (Supplementary Figure 7A VII-VIII). For CD133 and CD24 expression, we graded the samples as negative when <5% of membranous CD133 or CD24 was detected in cancer cells, whereas positive cases indicated \geq 5% of cancer cells expressed membranous CD133 or CD24 (Supplementary Figure 7B). Isotype IgG staining of CRC samples was used as a negative control of immunohistochemistry experiments (Supplementary Figure 7A IX).

Immunoblotting was performed as described⁶ with the following primary antibodies: Snail (catalog no. ab17732; Abcam), E-cadherin (catalog no. 4065; Cell Signaling), N-cadherin (catalog no. 610920; BD Biosciences, Franklin Lakes, NJ), Vimentin (catalog no. V6630; Sigma), IL8 (catalog no. AF-208-NA; R&D), CyclinD1 (catalog no. 2926; Cell Signaling), Akt (catalog no. 9272; Cell Signaling), Oct4 (catalog no. sc-9081; Santa Cruz Biotechnology), Sox2 (catalog no. ab75485; Abcam), β -actin (catalog no. MAB1501; Chemicon, Temecula, CA), and α -tubulin (catalog no. ab7291; Abcam). Secondary antibodies were as follows: bovine anti-rabbit IgG-HRP (catalog no. sc-2370; Santa Cruz Biotechnology), chicken anti-mouse IgG-HRP (catalog no. sc-2954; Santa Cruz Biotechnology), and chicken anti-goat IgG-HRP (catalog no. sc-2953; Santa Cruz Biotechnology). Immunoblots was visualized by the chemiluminescence detection system. Recombi-

nant transforming growth factor β 1 and IL8 were purchased from PeproTech Asia (Rehovot, Israel).

Immunofluorescent Assay

Cells were plated onto gelatin-coated glass coverslips overnight or by cytospin (for colonospheres) before fixation with 4% paraformaldehyde (Sigma) for 20 minutes at room temperature followed by PBS washes. Cells were permeabilized with 0.5% Triton X-100/PBS for 3 minutes at room temperature, washed with $1 \times$ PBS, and blocked in 5 mg/mL BSA (Sigma) in PBS for 30 minutes before probing with A33 (catalog no. sc-50522; Santa Cruz Biotechnology) primary antibodies followed by the rhodamine-tagged secondary antibodies (catalog no. AP-132R; Chemicon). Fluorescence images were visualized with a fluorescence microscope.

Flow Cytometry and Cell Sorting

Single cell suspensions were prepared, washed by cooled $1 \times$ PBS, and resuspended in incubation buffer (containing pH 7.2 PBS, 0.5% [wt/vol] BSA, and 2 mmol/L EDTA) on ice for 10 minutes for blocking. Cells were suspended in 1 mL incubation buffer to reach a final concentration of 2×10^5 cells/mL before stained with 0.5 g/mL of the following primary antibodies on ice for 30 minutes: anti-CD133-PE (AC133-2; MACS Miltenyi, Bergisch Gladbach, Germany), anti-CD24-FITC (ML5; Biolegend, San Diego, CA), anti-CD166 (MCA1926F; Serotec, Raleigh, NC), anti-CD44-PE (IM7; Biolegend), and CD44-FITC (BJ18; Biolegend). Aldefluor assay kit (Aldagen, Durham, NC) was used for the detection of aldehyde dehydrogenase activity according to the manufacturer's instructions. Data were collected by the FACSCalibur flow cytometer (Becton-Dickinson, Franklin Lakes, NJ) and analyzed with CellQuest software (BD Biosciences) or FlowJo software (TreeStar, San Carlos, CA). Cell debris was excluded from the analysis based on scatter signals, and fluorescent compensation was adjusted when double stained. For fluorescent-activated cell sorting in HT29 and HCT15 cells, cells were suspended in incubation buffer, stained with indicated primary antibodies (Figure 1B and C and Supplementary Figure 4A), and subjected to the FACS Aria (Becton-Dickinson) for single (CD133 or CD44) or double sorting (CD44/CD133 or CD44/CD24). Positive populations were defined compared with isotype control staining groups. The fluorescence-activated cell sorting plots and the resultant purity of sorted cells are shown in Supplementary Figure 3A–F. The resultant purities of sorted populations were confirmed (Supplementary Figure 3E–F), and only cells with $>80\%$ purity were applied for further analysis.

In Vitro Transwell Cell Migration, Matrigel Invasion, and Capillary Tube Formation Assay

Cell migration ability was evaluated by using a $8\text{-}\mu\text{m}$ filter membrane containing upper chamber

(Greiner Bio-One, Monroe, NC). Cells (1×10^5) suspended in 100 μL of culture medium containing 0.5% FBS were applied to the upper chamber of the device, and 600 μL of medium containing 0.5% FBS was added to the lower chamber. Cell invasiveness was examined by the Matrigel Basement Membrane Matrix invasion assay (Becton-Dickinson) according to the manufacturer's instructions. After 24 hours (48 hours in invasion assay) of incubation at 37°C , membranes were fixed with 4% paraformaldehyde (Sigma) for 20 minutes and then stained with 0.1% 4',6-diamidino-2-phenylindole (Sigma) solution for 10 minutes. Migrated cells were then visualized under an inverted microscope. For HMEC-1 chemotaxis assay, 0.5×10^5 cells were suspended in 100 μL DMEM basal medium in upper chamber, and conditional medium preabsorbed with 2 $\mu\text{g}/\text{mL}$ IL8 neutralizing antibody or normal IgG for 1 hour was added into lower chamber for 12 hours. In capillary tube formation assay, 1×10^4 human umbilical vein endothelial cells plated on a Matrigel-coated 96-well plate were incubated with combinational medium (conditional medium/EGM-2 = 3/1) or with combinational medium preabsorbed with 10 $\mu\text{g}/\text{mL}$ IL8 neutralizing antibody (R&D AF-208-NA) or normal IgG control (R&D AB-108-C) for 5 hours. The plate was then examined for capillary tube formation and photographed.

Statistical Analyses

Independent sample t tests were performed to compare the continuous variation of 2 groups, and the χ^2 test or Fisher exact test was applied for comparison of dichotomous variables. $P < .05$ was considered significant. All data are reported as mean \pm SEM.

References

1. Yang MH, Chiang WC, Chou TY, et al. Increased NBS1 expression is a marker of aggressive head and neck cancer and overexpression of NBS1 contributes to transformation. *Clin Cancer Res* 2006;12:507–515.
2. Yang MH, Wu MZ, Chiou SH, et al. Direct regulation of TWIST by HIF-1 α promotes metastasis. *Nat Cell Biol* 2008;10:295–305.
3. Huang CH, Yang WH, Chang SY, et al. Regulation of membrane-type 4 matrix metalloproteinase by SLUG contributes to hypoxia-mediated metastasis. *Neoplasia* 2009;11:1371–1382.
4. Chiou SH, Kao CL, Chen YW, et al. Identification of CD133-positive radioresistant cells in atypical teratoid/rhabdoid tumor. *PLoS ONE* 2008;3:e2090.
5. Wang HW, Trotter MW, Lagos D, et al. Kaposi sarcoma herpesvirus-induced cellular reprogramming contributes to the lymphatic endothelial gene expression in Kaposi sarcoma. *Nat Genet* 2004;36:687–693.
6. Huang TS, Hsieh JY, Wu YH, et al. Functional network reconstruction reveals somatic stemness genetic maps and dedifferentiation-like transcriptome reprogramming induced by GATA2. *Stem Cells* 2008;26:1186–1201.
7. Birnie R, Bryce SD, Roome C, et al. Gene expression profilin of human prostate cancer stem cells reveals a pro-inflammatory phenotype and the importance of extracellular matrix interactions. *Genome Biol* 2008;9:R83.

8. Shoemaker RH. The NCI60 human tumour cell line anticancer drug screen. *Nat Rev Cancer* 2006;6:813–823.
 9. Yang TP, Chang TY, Lin CH, et al. ArrayFusion: a web application for multi-dimensional analysis of CGH, SNP and microarray data. *Bioinformatics* 2006;22:2697–2698.
 10. Dennis G, Jr., Sherman BT, Hosack DA, et al. DAVID: Database for Annotation, Visualization, and Integrated Discovery. *Genome Biol* 2003;4:P3.
 11. Yang MH, Chang SY, Chiou SH, et al. Overexpression of NBS1 induces epithelial-mesenchymal transition and co-expression of NBS1 and Snail predicts metastasis of head and neck cancer. *Oncogene* 2007;26:1459–1467.
 12. Peinado H, Ballestar E, Esteller M, et al. Snail mediates E-cadherin repression by the recruitment of the Sin3A/histone deacetylase 1 (HDAC1)/HDAC2 complex. *Mol Cell Biol* 2004;24:306–319.
 13. Espineda CE, Chang JH, Twiss J, et al. Repression of Na,K-ATPase beta1-subunit by the transcription factor snail in carcinoma. *Mol Biol Cell* 2004;15:1364–1373.
-